DOI 10.5012/bkcs.2010.31.12.3658

Comparison of Binding Stoichiometry of [Ru(1,10-phenanthroline)$_2$dipyrido [3,2-*a*:2',3'-*c*]phenazine]$^{2+}$ and its *Bis*-derivative to DNA

Yoon Jung Jang,* Hyun Mee Lee, and Il-Bong Lee†

Department of Chemistry, Yeungnam University, Gyeongsan City, Gyeong-buk 712-749, Korea
**E-mail: jyj5014@ynu.ac.kr*
†Institute of Basic Science Research, Daegu Haany University, Yukok-dong, Gyeongsan City, Gyeong-buk 712-715, Korea
Received July 27, 2010, Accepted October 8, 2010

A new *bis*-Ru(II) complex, in which two [Ru(1,10-phenanthroline)$_2$dipyrido[3,2-*a*:2',3'-*c*]phenazine]$^{2+}$ were tethered by a 1,3-*bis*(4-pyridyl)propane linker, was synthesized and its binding mode and stoichiometry to DNA was investigated by optical spectroscopy including linear dichroism (LD) and fluorescence intensity measurement. The magnitude of the negatively reduced LD signal of the *bis*-Ru(II) complex in the dipyrido[3,2-*a*:2',3'-*c*]phenazine (DPPZ) ligand absorption region appeared to be similar compared to that in the DNA absorption region, which is considered to be a diagnostic for DPPZ ligand intercalation. The binding stoichiometry measured from its LD magnitude and enhanced fluorescence intensity corresponds to one ligand per three DNA bases, effectively violating the nearest neighbouring site exclusion model for classical DNA intercalation. This observation is in contrast with monomer analogue [Ru(1,10-phenanthroline)$_2$dipyrido[3,2-*a*:2',3'-*c*]phenazine]$^{2+}$, which is saturated at the DPPZ ligand to DNA base ratio of 0.25, or one DPPZ ligand per four nucleobases.

Key Words: *Bis*-Ru(II) complex, Intercalation, DNA, Light switch effect, Polarized spectroscopy

Introduction

The interaction of other molecules with DNA has been widely studied.[1] In particular, intercalation, the insertion of partially fused planar polycyclic heteroaromatic ligands between DNA base-pairs, is one of the typical binding modes. Ethidium is likely the most well-known intercalating compound. In the intercalation pocket, the molecular plane of ethidium is nearly parallel to the DNA base plane. Once an intercalation pocket is occupied, binding to the next pocket is prohibited; which makes, DNA becomes saturated at an [ethidium]/[DNA base] ratio of 0.25. This phenomenon is known as the "nearest neighbor site exclusion model".[2-4] The large dppz ligand of the [Ru(1,10-phenanthroline)$_2$dipyrido[3,2-*a*:2',3'-*c*]phenazine]$^{2+}$ (Figure 1a) complex (referred to as [Ru(phen)$_2$dppz]$^{2+}$; phen = phenanthroline, dppz = dipyrido[3,2-*a*:2',3'-*c*]phenazine) also intercalates with DNA. Insertion of the large dppz ligand seems to occur in the narrow minor groove, where the two bulky phenanthroline moieties are located,[5-6] although a few reports suggest that insertion takes place in the major groove.[7-9] Upon intercalation, the luminescence intensity of the Ru(II) complex increases remarkably due to the two close-lying metal-to-ligand charge transfer (MLCT) states, whose relative energies are sensitive to the polarity of the environment.[10-12] Enhancement in luminescence intensity of [Ru(phen)$_2$dppz]$^{2+}$ upon association with single-stranded DNA has also been reported.[13-15] In this paper, we report on the interaction of the newly synthesized *bis*-Ru(II)dppz complex (Figure 1b) with DNA. The luminescence intensity of the *bis*-Ru(II)dppz complex was also enhanced upon association with native, double-stranded DNA. The binding stoichiometry of this compound to DNA was 1:3, in contrast with the stoichiometry of 1:4 for classical intercalators such as ethidium and [Ru(phen)$_2$dppz]$^{2+}$.

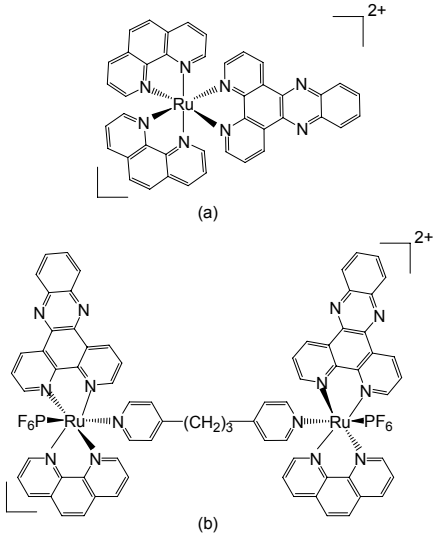

Figure 1. Chemical structures of *rac*-[dipyrido[3,2-*a*:2',3'-*c*] phenazine) (phenanthroline)$_2$Ru(II)]$^{2+}$ (a) and [μ-(linker) L$_2$(dipyrido[3,2-*a*:2',3'-*c*] phenazine)$_2$ (phenanthroline)$_2$Ru(II)$_2$]$^{2+}$, linker being 1,3-*bis*-(4-pyridyl)-propane (b).

Materials and Methods

Synthesis of [μ-(linker)(dipyrido[3,2-a:2',3'-c]phenazine)$_2$ (phenanthroline)$_2$Ru(II)$_2$]$^{2+}$, linker being 1,3-*bis*-(4-pyridyl)-propane. [Ru(phen)(dppz)Cl$_2$], was synthesized by a previously reported method.[16] The [Ru(phen)(dppz)Cl$_2$] (0.5 mmol, 0.3173 g) was dissolved in 10 mL EtOH:H$_2$O mixture (1:1, v/v), and then 0.25 mmol 1,3-*bis*(4-pyridyl)propane in a solution of 10 mL of an EtOH:H$_2$O mixture (1:1, v/v) was added. The solution was heated at reflux for seven days and cooled to room

temperature. The solvent was evaporated. The resulting reddish-brown residue was dissolved in EtOH and evaporated again. The residue was dissolved in hot water followed by centrifugation. The mixing of supernatant with aqueous ammonium hexafluorophosphate produced an orange solid. The solid was collected by filtration, washed with diethyl ether, and dried at 50 °C. The solid was dissolved in acetonitrile and subjected to alumina chromatograph (20 × 1 cm) twice with acetonitrile as the eluent. The orange band was collected and concentrated by evaporation and precipitated with diethyl ether. The light reddish-orange solid was collected by filtration, washed with diethyl ether, and dried in an oven (50 °C). The solid was then dissolved in acetone, and tetrabutylammonium chloride in acetone was added to obtain a water-soluble compound. The light reddish-orange solid was filtered, washed with diethyl ether, and dried in an oven (50 °C). All solvents used in this process were dried using standard procedures. All reactions were carried out under an inert atmosphere.

Yield: 90 mg. [μ-(bpp)$(PF_6)_2$(dppz)$_2$(phen)$_2Ru_2$] $(PF_6)_2$. Elemental analysis calcd (%) for $C_{73}H_{50}N_{14}P_4F_{24}Ru_2$ (1905.2734): C 46.02, H 2.65, N 10.29; found: C 46.01, H 2.34, N 10.26. ^{1}H-NMR ([μ-(bpp)$(PF_6)_2$(dppz)$_2$(phen)$_2Ru_2$] $(PF_6)_2$, 600 MHz, $CDCl_3$-*d*, 25 °C) δ 9.68 (dd, 4H), 8.71 (d, 2H), 8.66 (d, 1H), 8.58 (dd, 4H), 8.46 (t, 2H), 8.14 (t, 2H), 8.11 (d, 2H), 8.06 (dd, 4H), 8.03 (dd, 4H), 7.926 (t, 2H), 2.34 (t, 4H), 1.01 (t, 2H).

Materials and methods. Calf thymus DNA (referred to from now on as DNA) was purchased from Worthington (Lakewood, NJ, USA) and purified by dissolution (exhaustive shaking at 4 °C) in a 5.0 mM cacodylate buffer at pH 7.0, containing 100 mM NaCl and 1.0 mM EDTA, followed by several rounds of dialysis at 4 °C against 5.0 mM cacodylate buffer, pH 7.0. The latter buffer was used throughout this work. Other chemicals were purchased from Aldrich or Merck and used without purification. The mixing ratio, R, was defined as the ratio of the concentration of the dppz of the complex to the DNA base or phosphate concentration. Therefore, $R = 0.1$ indicates five *bis*-Ru(II) complexes (i.e., 10 dppz moieties) per 100 DNA bases or phosphate. The concentrations of DNA and of the *bis*-Ru(II)dppz complexes were determined spectrophotometrically using their proper extinction coefficients: $\varepsilon_{258nm} = 6700\ M^{-1}cm^{-1}$ for DNA. The extinction coefficient of the *bis*-Ru(II) complex was $\varepsilon_{372nm} = 29680 \pm 230\ M^{-1}cm^{-1}$ which was obtained from the average of three measured absorbance of the aqueous *bis*-Ru(II) complex solution whose concentration was carefully adjusted according to the well-known Beer Lambert law.

Linear dichroism (LD). Measurement of normal absorption spectra and linear dichroism (LD) spectra has been described elsewhere.[17] The ratio of measured LD to the isotropic absorption spectrum resulted in a wavelength-dependent quantity called the reduced LD (LD^r)[18-20] which is related to the angle between the DNA helical axis and the electronic transition moment of the DNA-bound Ru(II) complexes. The intensity of LD depends on the orientation factor and optical factor. The former requires the sample to be oriented in order to produces the LD signal. Thus, when other factors, including the gradient of flow in the flow oriented sample which was adopted in this study, salt concentration, temperature, and viscosity remain, the intensity of LD solely depends on the concentration of the DNA bound drug. Therefore, by comparing the LD intensity in the DNA absorption region and drug absorption region, the binding stoichiometry can be accurately determined to a reasonable extent. The measured LD^r was analyzed based on a detailed analysis of the electronic transition moment of the $[Ru(phen)_2dppz]^{2+}$ complex reported by Lincoln *et al.*[20]

Results and Discussion

Normal absorption and reduced linear dichroism. Figure 2 and Figure 3 show the absorption and LD^r spectra of the *bis*-Ru(II) complex bound to DNA at various mixing ratios. In all absorption ranges of the *bis*-Ru(II)dppz complex, hypochromism and red-shifts were apparent upon addition of DNA; these effects were especially pronounced in the dppz ligand absorption region. The shape of the absorption spectrum of the DNA-bound *bis*-Ru(II)dppz complex was independent of the mixing ratios, suggesting that the binding mode of the *bis*-Ru(II)dppz complex to DNA in the concentration range adopted in this study

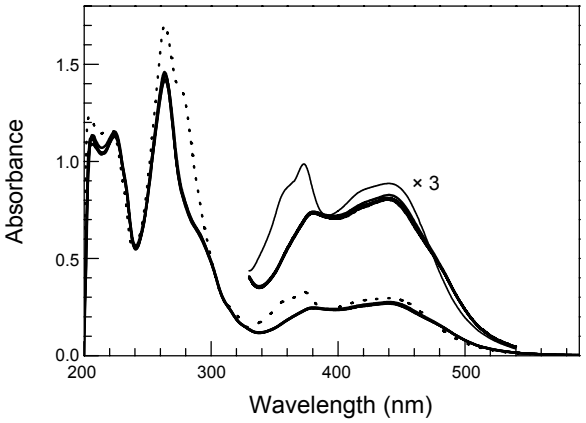

Figure 2. Absorption spectra of the *bis*-Ru(II) complex bound to DNA. [DNA] = 100 μM and [Ru(II) complex] = 2, 4, 6, 8, 10 μM. The absorption spectrum of the DNA was subtracted from that of the mixture and the spectra normalized to the highest concentration of Ru(II) complex. Dotted curve: Absorption spectrum of *bis*-Ru(II)dppz complex in the absence of DNA.

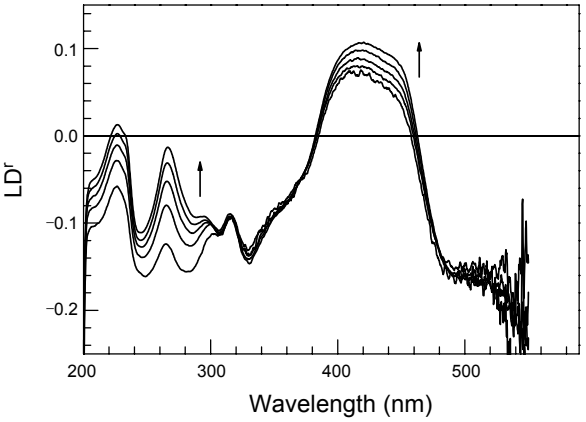

Figure 3. LD^r spectra of the *bis*-Ru(II) complex bound to DNA. [DNA] = 100 μM and [Ru(II) complex] = 2, 4, 6, 8, 10 μM. The spectrum changed in the direction of the arrows as the *bis*-Ru(II)dppz complex concentration increased.

is homogeneous. Furthermore, these observations suggested that all of the *bis*-Ru(II)dppz complex was bound to DNA. In the DNA absorption range, the LD^r, whose sign and magnitude are related to the angle between the electric transition moments of DNA-bound drugs and the DNA helical axis, appeared to be negative and relatively wavelength-independent, as expected.[18] Upon increase in the concentration of the *bis*-Ru(II)dppz complex, a positive and a clear peak near 254 nm was observed, originating from the absorption of the phenanthroline ligand. The LD^r signal in this region cannot be separated from that of the DNA bases, and therefore it will not be discussed further. The magnitude of the negative LD^r in the dppz absorption region (*ca*. 330 nm) was similar to that in the DNA absorption region, indicating that the molecular plane of the dppz ligand was parallel to the DNA base plane and perpendicular to the local DNA helical axis. The binding geometry estimated from the LD^r measurement and the large hypochromism and red-shift in the absorption spectra indicated that the dppz ligand intercalated between the DNA base pairs. The shape of the LD^r spectrum of the *bis*-Ru(II)dppz complex resembled that of the monomeric analogue, *rac*-$[Ru(phen)_2dppz]^{2+}$ (Figure 4), which is an intermediate between the spectra of the Δ- and Λ-enantiomers of the $[Ru(phen)_2dppz]^{2+}$ monomers reported by Lincoln and coworkers.[20] The characteristic bisignate LD^r spectra of both enantiomers above ~ 400 nm have been assigned to a complicated arrangement of the MLCT band with respect to the DNA helical axis.

The light switch effect. It is well known that the luminescence intensity of the $[Ru(phen)_2dppz]^{2+}$ complex is enhanced considerably upon association with DNA.[13-15] This phenomenon has been known as the "lightswitch effect". Since the origin of this effect is the removal of the water molecules surrounding the $[Ru(phen)_2dppz]^{2+}$ complex, it has often been regarded as an indication of intercalation of the dppz ligand. As shown in Figure 5, the luminescence intensities of both the *bis*-Ru(II)dppz and *rac*-$[Ru(phen)_2dppz]^{2+}$ complexes increase upon binding to DNA. The intensity at the maximum is comparable, suggesting that the dppz ligands of both complexes are protected from the water molecules to similar extents. The maximum is reached at a mixing ratio of 0.25 ~ 0.3 for the *rac*-$[Ru(phen)_2dppz]^{2+}$ complex. Further increase in the mixing ratio results in a slight decrease in the luminescence intensity by self-quenching. In contrast, the mixing ratio at the maximum luminescence intensity is not clear for the *bis*-Ru(II)dppz complex and no evidence for self-quenching was found.

Binding stoichiometry: the Job plot. The binding stoichiometry of the Ru(II) complexes may be determined from the Job plot, as shown in Figure 6. Association of the *bis*-Ru(II)dppz complex with DNA resulted in enhanced luminescence intensity, as was also observed for $[Ru(phen)_2dppz]^{2+}$ monomers. In the $[Ru(phen)_2dppz]^{2+}$ monomer case, the luminescence intensity increased almost proportionally with increasing mole fraction. The maximum was found at a $[Ru(phen)_2dppz]^{2+}$ mole fraction of 0.2 corresponding to one intercalated dppz ligand for every two base pairs in accordance with the nearest neighbor

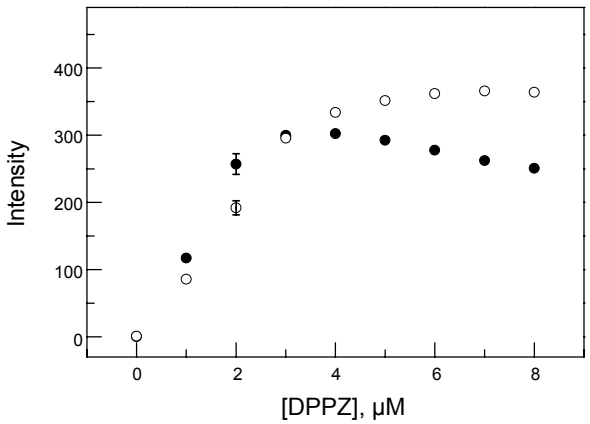

Figure 5. Enhancement in luminescence intensity of the *bis*-Ru(II)dppz complex (opened circles) and *rac*-$[Ru(phen)_2dppz]^{2+}$ (closed circles) as concentration increases. [DNA] = 10 μM. The concentration of the Ru(II) complexes is in the dppz unit. Excitation and emission wavelengths were 440 and 606 nm, respectively. Representative error bars which denote the standard deviation for three measurements are shown.

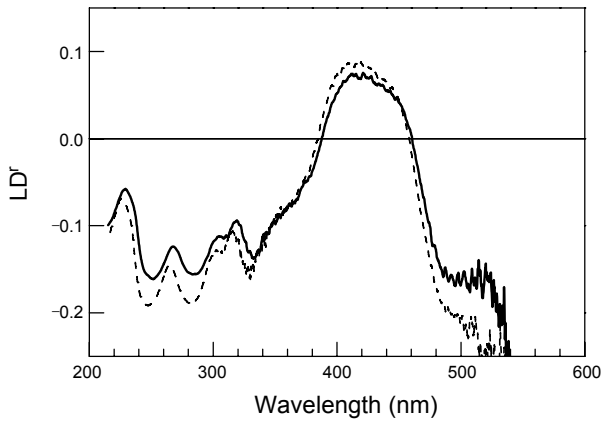

Figure 4. Comparison of LD^r spectra of the *bis*-Ru(II)dppz complex (solid curve) and *rac*-$[Ru(phen)_2dppz]^{2+}$ (dashed curve) associated with DNA. [DNA] = 100 μM, [*bis*-Ru(II)dppz complex] = 2 μM and [*rac*-$[Ru(phen)_2dppz]^{2+}$] = 4 μM.

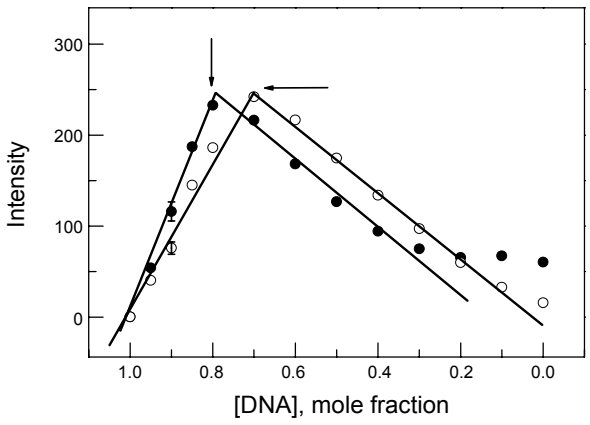

Figure 6. The Job plot for the *bis*-Ru(II)dppz complex-DNA (opened circles) and the *rac*-$[Ru(phen)_2dppz]^{2+}$-DNA mixture (closed circles). The total concentration was 10 μM. Excitation and emission wavelengths were 440 and 606 nm, respectively. Representative error bars which denote the standard deviation for three measurements are shown.

site exclusion model. Further increase in the mole fraction of $[Ru(phen)_2dppz]^{2+}$ resulted in a decrease in the luminescence intensity. It is note-worthy that a rapid change in the slope was also found at a mole fraction of ~0.7, which corresponds to two $[Ru(phen)_2dppz]^{2+}$ complexes per one DNA base. The Job plot was constructed for the *bis*-Ru(II)dppz complex by mole fraction of the intercalated dppz ligand. To our surprise, the maximum was found at a mole fraction of 0.25 ~ 0.3 intercalated dppz. The stoichiometry corresponded to one intercalation per 2.3 ~ 3 DNA bases, which cannot be explained by the nearest neighbor site exclusion model. This stoichiometry can be confirmed by the linear dichroism (LD) spectrum (Figure 7). The LD spectrum is active only for the oriented chromophore. Therefore, the magnitude of LD in the drug absorption region reflects the concentration of the DNA-bound drug. As the concentration of $[Ru(phen)_2dppz]^{2+}$ increased at a fixed DNA concentration, the magnitude of the LD proportionaly increased. The maximum LD magnitude was found at a mixing ratio of 0.2 ~ 0.25. In addition to the Job plot, this observation provides evidence for the binding stoichiometry of one dppz per four DNA bases, or the nearest neighbor site exclusion model in the $[Ru(phen)_2dppz]^{2+}$ complex case. The magnitude of the LD tended to decrease when the concentraion of $[Ru(phen)_2dppz]^{2+}$ was further increased. One possible explanation is that when all possible intercalation sites were saturated, surface binding of the $[Ru(phen)_2dppz]^{2+}$ complex could conceivably have occured, thereby making the DNA more flexible. In contrast, the maximum LD intensity was found at a mixing ratio of ~ 0.35 for the *bis*-Ru(II)dppz complex, corresponding to one intercalated dppz per three DNA bases, again violating the nearest neighbor site exclusion model but agreeing with the results obtained from the Job method.

The binding mode. Given that: i) the magnitude of the LD^r in the dppz absorption region is comparable to that of the DNA absorption region when the *bis*-Ru(II) complex is associated with DNA; ii) the shape of the LD^r spectrum of the DNA-*bis*-Ru(II) adduct resembles that of the DNA-$[Ru(phen)_2dppz]^{2+}$ monomer adduct at the same dppz concentration; and iii) the increase in luminescence intensity upon binding to DNA is similar for both Ru(II) complexes, it is conclusive that both dppz ligands of the *bis*-Ru(II) complex intercalate between DNA base pairs. Interactions of other structurally related *bis*-Ru(II) complexes with DNA have been reported.[21-22] For instance, interaction of the two Ru(II)dppz units tethered by a 4,4'-dipyridyl-1,5-pentane linker with DNA has been investigated through spectroscopic and thermodynamic studies showing that at least one of the two dppz ligands intercalates between DNA base-pairs.[22] Although the linker used in this study, 4,4'-dipyridyl-1,3-propane, is significantly shorter, it may be long enough to make room for two DNA base pairs (~ 6.8 Å thick) between the two parallel dppz molecular planes when fully extended. If the linker of the *bis*-Ru(II) complex is fully extended to hold two base pairs between the dppz ligands (Figure 8), the binding stoichiometry should be one dppz ligand per four DNA bases, obeying the nearest neighbor site exclusion model as observed for the mono-intercalating *rac*-$[Ru(phen)_2dppz]^{2+}$ complex. However, for the *bis*-Ru(II) complex, the binding stoichiometry appeared to be one intercalated dppz per 2.3 ~ 3 DNA bases. In order for this binding stoichiometry to be possible, insertion of the second dppz ligand at the intercalation site right next to the first dppz intercalation site must be allowed, as shown in Figure 8. The binding models in accordance with the "nearest

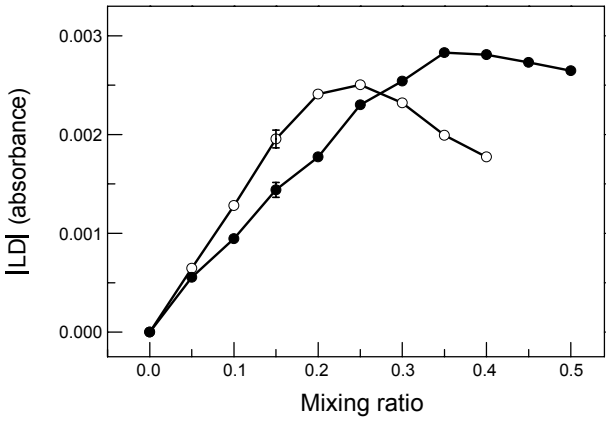

Figure 7. Changes in LD intensity at 484 nm relative to the mixing ratio. [DNA] = 100 μM. In both panels, the concentration of the Ru(II) complex is denoted by the dppz unit. Open circles represent *rac*-$[Ru(phen)_2dppz]^{2+}$ and closed circles the *bis*-Ru(II)dppz complex. Representative error bars which denote the standard deviation for three measurements are shown.

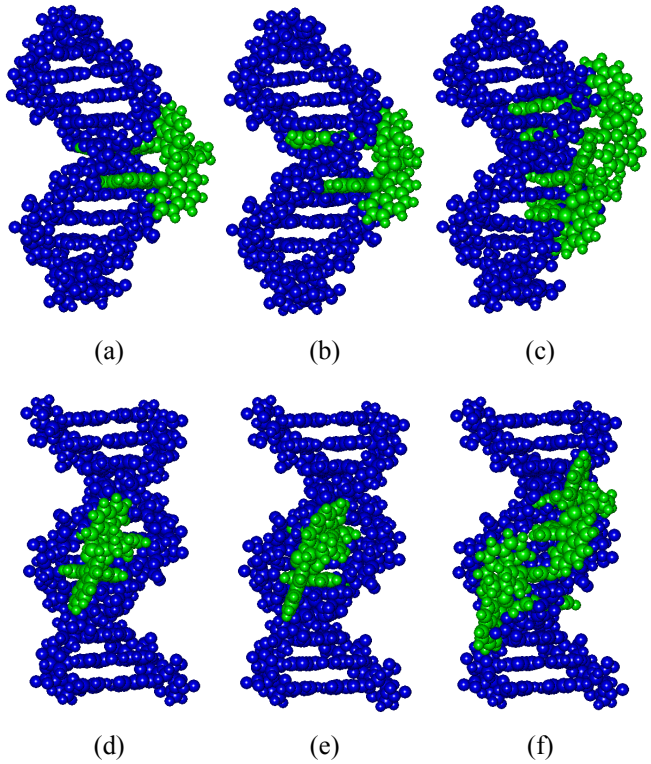

Figure 8. Illustrative diagram for intercalation of dppz to 2 consecutive intercalation pockets (a: side view and d: viewed from the minor groove) and to every other pocket (b: side view and e: viewed from the minor groove). The latter obeying the nearest neighbor site exclusion model. Two Ru(II) complexes can consecutively bound to DNA (c: side view and f: viewed from the minor groove) showing that the binding stoichiometry presented in the text is possible.

side exclusion model" are compared in the same Figure (Figures 8b and e). The conformation of both DNA and the Ru(II) complex are not much strained. A vacant site may follow the two continuous dppz intercalated pockets as shown in Figures 8c and f, which also present the possibility of the enough space for the two Ru(II) complex intercalate consecutively.

Acknowledgments. The author acknowledge support for the postdoctoral fellowship conferred by the Korea Research Foundation (Grant no. C00125, 2009).

References

1. Norden, B.; Lincoln, P.; Turite, E. *New York* **1996**, 177-252.
2. Crothers, D. M. *Biopolymers* **1968**, *6*, 575-584.
3. Bond, P. J.; Langridge, R. R.; Jennette, K. W.; Lippard, S. J. *Proc. Ntal. Acad. Sci. USA* **1975**, *72*, 4825-4829.
4. Hogan, M.; Dattagupta, N.; Crothers, D. M. *Biochemistry* **1979**, *18*, 280-288.
5. Dupureur, C. M.; Barton, J. K. *J. Am. Chem. Soc.* **1994**, *116*, 10286-10287.
6. Holmlin, R. E.; Stemp, E. D. A.; Barton, J. K. *Inorg. Chem*. **1998**, *37*, 29-34.
7. Choi, S.-D.; Kim, M.-S.; Kim, S. K.; Lincoln, P.; Tuite, E.; Nordén, B. *Biochemistry* **1997**, *36*, 214-223.
8. Tuite, E.; Lincoln, P.; Nordén, B. *J. Am. Chem. Soc.* **1997**, *119*, 239-240.
9. Greguric, A.; Greguric, I. D.; Hambley, T. W.; Aldrich-Wright, J. R.; Collins, J. G. *J. Chem. Soc., Dalton Trans*. **2002**, 849-855.
10. Olson, E. J. C.; Hu, D.; Hörmann, A.; Jonkman, A. M.; Arkin, M. R.; Stemp, E. D. A.; Barton, J. K.; Barbara, P. F. *J. Am. Chem. Soc.* **1997**, *119*, 11458-11467.
11. Önfelt, B.; Lincoln, P.; Nordén, B.; Baskin, J. S.; Zewail, A. H. *Proc. Natl. Acad. Sci. USA* **2000**, *97*, 5708-5713.
12. Coares, C. G.; Olofsson, J.; Coletti, M.; McGarvey, J. J.; Önfelt, B.; Lincoln, P.; Nordén, B.; Tuite, E.; Matousek, P.; Parker, A. W. *J. Phys. Chem. B* **2001**, *105*, 12653-12664.
13. Coates, C. G.; McGarvey, J. J.; Callaghan, P. L.; Coletti, M.; Hamilton, J. G. *J. Phys. Chem. B* **2001**, *105*, 730-735.
14. Moon, S. J.; Kim, J. M.; Choi, J. Y.; Kim, S. K.; Lee, J. S.; Jang, H. G. *J. Inorg. Biochem*. **2005**, *99*, 994-1000.
15. Kim, J. M.; Lee, J.-M.; Choi, J. Y.; Lee, H. M.; Kim, S. K. *J. Inorg. Biochem*. **2007**, *101*, 1386-1393.
16. Hirot, C.; Lincoln, P.; Nordén, B. J. *J. Am. Chem. Soc.* **1993**, *115*, 3448-3454.
17. Jang, Y. J.; Kwon, B.-H.; Choi, B.-H.; Bae, C. H.; Seo, M. S.; Nam, W. W.; Kim, S. K. *J. Inorg. Biochem.* **2008**, *102*, 1885-1891.
18. Nordén, B.; Kurucsev, T. *J. Mol. Recognit.* **1994**, *7*, 141-155.
19. Nordén, B.; Kubista, M.; Kurucsev, T. *Q. Rev. Biophys*. **1992**, *25*, 51-170.
20. Lincoln, P.; Broo, A.; Nordén, B. *J. Am. Chem. Soc.* **1996**, *118*, 2644-2653.
21. Pierard, F.; Kirsch-De Mesmaeker, A. *Inorg. Chem. Commun*. **2006**, *9*, 111-126.
22. Metcalfe, C.; Haq, I.; Thomas, J. A. *Inorg. Chem*. **2004**, *43*, 317-323.